

Characterisation of lensing selection effects for LISA massive black hole binary mergers

Giulia Cusin^{1*}, Nicola Tamanini²

¹*Université de Genève, Département de Physique Théorique and Centre for Astroparticle Physics, 24 quai Ernest-Ansermet, CH-1211 Genève 4, Switzerland*

²*Max Planck Institute for Gravitational Physics (Albert Einstein Institute), Am Mühlenberg 1, Potsdam-Golm, 14476, Germany*

21 May 2021

ABSTRACT

We present a method to include lensing selection effects due to the finite horizon of a given detector when studying lensing of gravitational wave (GW) sources. When selection effects are included, the mean of the magnification distribution is shifted from one to higher values for sufficiently high-redshift sources. This introduces an irreducible (multiplicative) bias on the luminosity distance reconstruction, in addition to the typical source of uncertainty in the distance determination. We apply this method to study lensing of GWs emitted by massive black hole binary mergers at high redshift detectable by LISA. We estimate the expected bias induced by selection effects on the luminosity distance reconstruction as function of cosmological redshift, and discuss its implications for cosmological and astrophysical analyses with LISA. We also reconstruct the distribution of lensing magnification as a function of the observed luminosity distance to a source, that is the observable quantity in the absence of an electromagnetic counterpart. Lensing provides the dominant source of errors in distance measurements of high-redshift GW sources. Its full characterisation, including the impact of selection effects, is of paramount importance to correctly determine the astrophysical properties of the underlying source population and to be able to use gravitational wave sources as a new cosmological probe.

Key words: gravitational waves, compact binaries, gravitational lensing

1 INTRODUCTION

The *Laser Interferometer Space Antenna* (LISA), an ESA-led space mission with launch expected for 2034, will open a new low-frequency window in the gravitational-wave (GW) spectrum (Amaro-Seoane et al. 2017), which should lead to the detection of a plethora of new GW sources promising to double the recent revolutionary discoveries achieved at high frequencies by the LIGO-Virgo interferometers (Abbott et al. 2016c,b,a, 2017c,d,b,a, 2019, 2020). Among all the different GW sources that LISA will observe, the merger of massive black hole binaries (MBHB) in the $10^4 - 10^7$ solar mass range is considered one of the key targets of the mission (Klein et al. 2016). Their de-

tection will allow us to probe for the first time the true nature of the massive dark objects found at the centers of galaxies, testing in this way the hypothesis that MBHBs come from the inevitable outcome of galaxy assembly, and consequently unveiling the origin and growth history of MBHBs at high redshift (Haehnelt 1994; Kauffmann & Haehnelt 2000; Volonteri, Haardt & Madau 2003; Enoki et al. 2004; Sesana et al. 2005; Micic et al. 2007; Barausse 2012; Colpi 2014; Umeda et al. 2016; Valiante et al. 2016).

MBHB mergers will be detected by LISA up to very high redshift (Klein et al. 2016), possibly up to $z \sim 20$ if any of them can be formed so early in the cosmic history. Intervening matter along the line of sight between the source and the observer will lens the GW signal, changing some of the properties from the emitted to the observed waveform, in particular magnifying/de-magnifying its am-

* giulia.cusin@unige.ch

plitude and consequently shifting the measured value of the luminosity distance, hence biasing the inferred source-frame chirp mass¹. These effects will be particularly relevant for the few LISA MBHB events that will appear strongly lensed (Sereno et al. 2010, 2011).

In this study we present a method to estimate the effect of lensing on the luminosity distance of high redshift GW astrophysical sources, such as LISA MBHBs, including for the first time selection effects due to the finite horizon of the GW detector. The impact of gravitational lensing on the distance measurement for MBHBs was already pointed out by Holz & Hughes (2005); Hilbert, Gair & King (2011); Hirata, Holz & Cutler (2010a); Shang & Haiman (2010), where it is estimated that lensing will introduce an insurmountable error of a few percent on the distance estimate, for each individual high redshift binary system. In these works, the effect of lensing is directly estimated from the distribution of lensing magnification as a function of cosmological redshift, typically obtained from ray-tracing simulations (e.g. Sato et al. (2009); Takahashi et al. (2011)). However a realistic GW detector has a finite sensitivity: magnified sources are on average easier to detect than de-magnified ones and this affects the distribution of lensing magnification of an observed source sample. These effects, hereafter dubbed *selection effects*, are usually neglected when estimating the lensing-induced uncertainty on the cosmological distance measurement from high-redshift GW sources.

When selection effects are included, the mean of the magnification distribution is shifted from 1 as we go farther in redshift. This introduces an irreducible (multiplicative) bias on the distance reconstruction, independent of the sample size. We apply this method to estimate the effect of lensing on a population of MBHB mergers detectable by LISA and we compute bias and uncertainty of the distance estimator as functions of cosmological redshift. We also compute the distribution of lensing magnification as a function of the observed luminosity distance (using the entire source population), that is the observable quantity in the absence of an EM counterpart.

Our results have direct impact on cosmological and astrophysical investigations made with LISA. MBHBs mergers can indeed be used as *standard sirens* (Schutz 1986) to probe the rate of expansion of the universe at high-redshift whenever an electromagnetic (EM) counterpart can be identified. Recent forecasts show that LISA, in combination with suitable EM facilities, will provide few MBHB standard sirens per year up to $z \simeq 8$ (Tamanini et al. 2016), yielding stringent constraints at high redshift not only on Λ CDM but also on possible deviations from it (Caprini & Tamanini 2016; Cai, Tamanini & Yang 2017; Belgacem et al. 2019; Calcagni et al. 2019a,b; Corman,

¹ From the waveform one can extract the redshifted chirp mass of the source. If the distance reconstruction is biased, also redshift associated to that distance (by fixing a reference cosmological model) is biased, hence the reconstruction of the source-frame chirp mass is biased as well.

Escamilla-Rivera & Hendry 2020; Speri et al. 2020). On the other hand, high-redshift MBHB mergers can also be used to test the formation, evolution and environment of MBHs (Sesana, Volonteri & Haardt 2007; Sesana et al. 2011; Colpi et al. 2019; Mukherjee, Wandelt & Silk 2020), and thus shed light on the astrophysical properties of their population across cosmic time. Here we show how lensing selection effects affect these investigations, discussing in particular the impact that our results have on the cosmological and astrophysical analyses that have been proposed for LISA.

In what follows we set $c = 1$, but keep the gravitational constant G . We assume vanishing spatial curvature and we set the present scale factor, $a_0 = 1$. We set Λ CDM as our fiducial cosmology with cosmological parameters taken from Takahashi et al. (2011).

2 INCLUSION OF SELECTION EFFECTS

We follow the derivation of Cusin, Durrer & Dvorkin (2019). A realistic GW detector has a limiting strain sensitivity, usually cast as an SNR limit, ρ_{lim} . A source is detected if $\rho \geq \rho_{\text{lim}}$, where the SNR ρ is defined by (Finn & Chernoff 1993)

$$\rho^2 = 4 \int \frac{|h(f)|^2}{S_n(f)} df = \int \rho^2(f) df. \quad (1)$$

Here $S_n(f)$ is the noise of the detector at frequency f , see e.g. Maggiore (2007).

If an event is magnified by $\mu > 1$ we could see it even if without magnification its SNR is below threshold. In other terms, denoting with ρ_{lim} the SNR threshold for detection in the absence of lensing, in general in the presence of magnification $\mu > 1$, the threshold for detection lowers to $\rho_{\text{lim}}/\sqrt{\mu}$. It follows that in the presence of magnification, the total number of objects which we expect to see from a redshift bin dz is given by the following convolution (Cusin, Durrer & Dvorkin 2019)

$$dN_{\text{obs}}(z, \rho_{\text{lim}}) = \int_0^\infty d\mu p(\mu, z) dN(\mu, z), \quad (2)$$

where $p(\mu, z)$ is the distribution of lensing magnification as a function of cosmological redshift and

$$dN(\mu, z) \equiv dz \int_{\rho_{\text{lim}}/\sqrt{\mu}}^\infty N(z, \rho) d\rho, \quad (3)$$

is the number of sources that we see from redshift z in the presence of magnification μ and $N(z, \rho)$ is the number density of sources as function of redshift and SNR ρ .² The mean amplification of a source at redshift z is

$$\langle \mu \rangle(z) = \frac{\int_0^\infty d\mu \mu p(\mu, z) dN(\mu, z)}{\int_0^\infty d\mu p(\mu, z) dN(\mu, z)}. \quad (4)$$

² In Eq. (3) we have denoted with ρ the SNR of a source computed assuming no lensing effects.

Note that (4) is the first moment of the probability distribution of magnification as seen by the detector (i.e. with selection effects included)

$$\mathcal{P}_z(\mu, z) \equiv \mathcal{C} p(\mu, z) \frac{d\mathcal{N}(\mu, z)}{dz}, \quad (5)$$

where \mathcal{C} is a normalization constant. Eq. (5) depends on three basic ingredients: *i*) distribution of magnification $p(\mu, z)$, *ii*) distribution of sources as a function of redshift and luminosity (or analogously ρ) *iii*) sensitivity curve of a given experiment.

In the absence of an EM counterpart, we do not know the cosmological redshift of a GW event. We usually infer it by assuming that the observed luminosity distance is the one of the background universe without magnification. In the presence of magnification, the relation between observed and cosmological luminosity distance is given by $D_{\text{obs}}(z, \mu) \equiv D(z)/\sqrt{\mu}$. One can rewrite (2) and (4) as functions of the observed luminosity distance extracted from observations, using their relation in terms of magnification. Then in full analogy with eq. (5), the probability distribution of magnification at the detector, as a function of the observed luminosity distance of the source, is given by (Cusin, Durrer & Dvorkin 2019)

$$\mathcal{P}_{\text{obs}}(\mu, D_{\text{obs}}) \equiv \mathcal{C} p(\mu, D_{\text{obs}}) \frac{d\mathcal{N}(\mu, D_{\text{obs}})}{dD_{\text{obs}}}, \quad (6)$$

where \mathcal{C} is a constant of normalization and $d\mathcal{N}(\mu, D_{\text{obs}})/dD_{\text{obs}}$ is the number of sources observable at observed distance D_{obs} if the magnification is μ , explicitly given by (Cusin, Durrer & Dvorkin 2019)

$$\frac{d\mathcal{N}(\mu, D_{\text{obs}})}{dD_{\text{obs}}} = \frac{\sqrt{\mu}}{D'(z(D_{\text{obs}}, \mu))} \int_{\rho_{\text{lim}}/\sqrt{\mu}}^{\infty} N(\rho, z) d\rho, \quad (7)$$

where $z = z(D_{\text{obs}}, \mu)$ and a prime denotes a derivative with respect to the argument.

3 LUMINOSITY DISTANCE ESTIMATOR

Let us assume that we observe a sample of sources with EM counterpart. From each observed event we extract a luminosity distance D_{obs} and redshift z , and for each source, the observed and cosmological distance are related through $D^2 = \mu D_{\text{obs}}^2$. We bin sources in redshift and we associate to each bin z an average *observed* luminosity distance as

$$\bar{D}_{\text{obs}}^2 \equiv \left[\frac{1}{N(z)} \sum_{i=1}^N D_{\text{obs},i}^2 \right], \quad (8)$$

where $N(z)$ is the number of sources in the bin z .

We write a (formal) expression for the true (unlensed) luminosity distance at a given redshift as

$$\hat{D}^2(z) = \frac{1}{N(z)} \sum_{i=1}^N \mu_i D_{\text{obs},i}^2 \simeq \mu(z) \bar{D}_{\text{obs}}^2. \quad (9)$$

To go to the last equality in eq. (9) we used the fact that

the magnification of a single source is not observable and we replaced $\mu_i \rightarrow \mu(z)$ where $\mu(z)$ is a stochastic parameter which follows the distribution $\mathcal{P}_z(\mu, z)$. We stress that (9) has to be interpreted as a formal expression: only its average and higher moments can be computed from data and theoretical inputs such as the PDF of magnification computed from ray-tracing simulations. Denoting with $\langle \dots \rangle$ the average of a function of μ computed with the distribution $\mathcal{P}_z(\mu, z)$, we have that

$$\langle \hat{D}^2(z) \rangle = \langle \mu(z) \rangle \bar{D}_{\text{obs}}^2, \quad (10)$$

where $\langle \mu(z) \rangle$ is explicitly given by (4). We observe that the quantity $\langle \mu(z) \rangle$ is traditionally assumed to be one, see e.g. Hirata, Holz & Cutler (2010b); Holz & Linder (2005). However, once selection effects due to the sensitivity curve of a given observatory are included, flux conservation is not enforced anymore and in general $\langle \mu(z) \rangle \neq 1$, hence this amplification factor needs to be added to get an unbiased estimate of the cosmological distance. We also stress that in eq. (10) two independent average procedures are involved: an arithmetic mean to compute the average distance of the sample and a stochastic mean with the magnification PDF.³

To estimate the uncertainty on the determination of the cosmological distance, we follow Hirata, Holz & Cutler (2010b) and we compute a variance given by the inverse of the Fisher information. We get (see appendix for details)

$$\sigma(\ln \hat{D}^2) \simeq \frac{1}{\sqrt{I(x)}}, \quad (11)$$

where $x \equiv \ln \mu$ and $I(x)$ is the Fisher information

$$I(x) \equiv N(z) \int \mathcal{P}_z(x, z) \left[\frac{d}{dx} \ln \mathcal{P}_z(x, z) \right]^2 dx. \quad (12)$$

Notice that while in Hirata, Holz & Cutler (2010b) the Fisher information is computed from the distribution of magnification $p(x, z)$ which depends only on the matter distribution of the Universe, we compute the Fisher information from the distribution, $\mathcal{P}_z(x, z)$, which contains selection effects specific to a given observatory.

The reason why we estimate the variance of (9) using its Cramer-Rao bound instead of computing the second moment of the estimator with the PDF of μ is that the latter, namely σ_μ , is a divergent quantity: the PDF decays as μ^{-3} at high μ , hence σ_μ has an ultraviolet logarithmic divergence. However, this divergence is not physical and it is a consequence of the fact that, to predict the high-magnification tail of the magnification distribution, we are artificially assuming that ray optics is a good approximation at any scale. Realistically, wave effects appear below

³ Note that the actual bias on the distance is given by $\langle \mu^{1/2}(z) \rangle$. We decide however to work with a quadratic quantity in eq. (9) to stress the effect of lensing selection, as the bias on the distance square is identically one if selection effects are not accounted for.

a given frequency-dependent scale and regularise this divergence effectively introducing a frequency-dependent ultraviolet cut-off in μ . To describe this effect properly, one should re-run a ray-tracing simulation introducing diffraction effects below a given frequency dependent scale. Such an investigation is outside the scope of the present study. Instead of introducing artificial cut-offs in the computation of the the second moment of the magnification distribution, we decided here to estimate the variance of the estimator using its Cramer-Rao bound.⁴

In the absence of an EM counterpart, we have access only to the observed luminosity distance D_{obs} of a source. If we have a set of N sources with observed distances distributed in a bin with mean D_{obs} , the average (true, cosmological) luminosity distance associated to the sample is given by

$$\langle \hat{D}^2(D_{\text{obs}}) \rangle = \langle \mu(D_{\text{obs}}) \rangle D_{\text{obs}}^2, \quad (13)$$

where $\langle \mu(D_{\text{obs}}) \rangle$ is the mean magnification associated to the distribution of magnification \mathcal{P}_{obs} as function of the observed distance defined in eq. (6). Eq. (13) gives an estimate of the (real) luminosity distance of a sample as a function of the observed luminosity distance, and corresponds to eq. (10), computed as function of the sample observed distance (instead of redshift). The uncertainty associated to the estimator (13) is given by eq. (11) where the Fisher information (12) has to be computed using the probability distribution (6).

In the rest of this paper we will often refer to the average magnification $\langle \mu \rangle \neq 1$ as bias on distance estimator, understanding that if the presence of magnification is not accounted for, we get a biased reconstruction of a source luminosity distance. We stress that this is somehow an abuse of language: the estimator formally defined in (9) is actually unbiased by construction.

4 RESULTS FOR LISA

We apply the analysis presented in the previous section to the case of MBHBs detectable by LISA. Our first goal is to compute the bias $\langle \mu^{1/2}(z) \rangle$ and the uncertainty of the distance estimator \hat{D} , for the full population of MBHBs and the sub-population with EM counterpart. Three ingredients enter the computation: (i) The distribution of magnification as a function of cosmological redshift $p(\mu, z)$, which we take from the high-resolution ray-tracing simulations of Takahashi et al. (2011). The box size of the simulation is $50h^{-1}\text{Mpc}$ with 1024^3 particles, the mean particle separation is $50h^{-1}\text{kpc}$, and the softening length of $h^{-1}\text{kpc}$. The resolution is such that the simulation predicts both the low magnification contribution to the PDF due to the large scale structure, and the strong lensing

⁴ We checked that estimating the variance directly from (9) adding by hand an upper cut-off in μ gives results in qualitative agreement with the Cramer-Rao estimate (e.g. within 8% if we artificially fix this cut-off at $\mu = 5$).

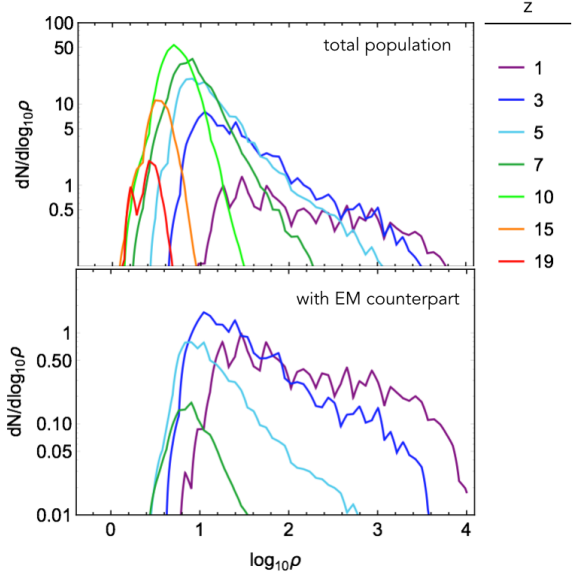


Figure 1. Number of events per unit redshift, for the total population and the sub-population with EM counterpart. Each line corresponds to the number of events in a redshift bin $z \pm 0.5$ and the values of z are listed in the legend on the right of the figure. We fixed an observation time $T_{\text{obs}} = 1$ year. The number of events increase linearly with T_{obs} .

high-magnification tail up to halo scales, which is particularly relevant for our analysis. The simulation does not consider the effect of baryons, which typically enhance the strong magnification tail. This means that the results we will get using the simulations of Takahashi et al. (2011) for lensing selection effects are rather conservative. We also observe that GW in the LISA band are insensitive to sub-galactic structures as diffraction becomes very effective on those scales (Takahashi & Nakamura 2003). (ii) The LISA strain noise curve, which we take from Amaro-Seoane et al. (2017); Robson, Cornish & Liu (2019). We include the contribution from galactic binaries to the noise curve, assuming a nominal duration of the mission of 4 years. To estimate the SNR in eq. (1), we employ the phenomenological inspiral-merger-ringdown waveform model known as PhenomA (Ajith et al. 2007). While more accurate models now certainly exist, which include spin-precession and other effects, for our purposes PhenomA is sufficiently accurate to estimate the SNR, and in fact gives results compatible with the ones of Klein et al. (2016); Tamanini (2017) for the number of events above threshold. (iii) The astrophysical model for MBHB distribution. We use here for definiteness the catalogues used in Klein et al. (2016), based on the MBHB populations of Barausse (2012). Note that although there are more recent studies yielding updated populations of MBHBs for LISA (e.g. Salcido et al. (2016); Bonetti et al. (2019); Katz et al. (2020); Dayal et al. (2019)), for our case study we choose to work with the catalogues used in Klein et al. (2016) since for these we can also retrieve the fraction of the population with

EM counterpart from [Tamanini et al. \(2016\)](#); [Tamanini \(2017\)](#). We focus in particular on the “popIII” population model based on light growth seeds for MBHs, since it is more affected by lensing selection effects, as we will show below. In what follows all results will refer to this model, unless otherwise specified. We provide in fact results for the other two “Q3” heavy-seed MBH population models considered in [Klein et al. \(2016\)](#) whenever they are relevant, and review their cases in more details in the discussion below. The distribution of MBHB mergers in the popIII model as a function of SNR and redshift is presented in Fig. 1, for both the full population and the sub-population with EM counterpart.

The distribution of magnification for LISA, once selection effects are included, eq. (4), is shown in the bottom panel of Fig. 2. Each line corresponds to a cosmological redshift and it is obtained multiplying the distribution of magnification of the ray-tracing simulation of [Takahashi et al. \(2011\)](#) by the number of objects visible with LISA from a given redshift, as a function of magnification, eq. (3). This latter is shown in the top panel of Fig. 2, for different redshifts. The number of events visible from a given redshift is a monotonically increasing function of magnification, and it reaches a plateau at the value of magnification for which all sources from that redshift have been observed. As expected, the value of magnification at which the plateau is reached is a monotonically increasing function of redshift. It follows that selection effects are more important for high redshift sources than for low redshift ones.

Finally we compute the bias and the uncertainty of the distance estimator \hat{D} . We observe that the bias is independent of the sample size while the variance scales as $\propto 1/\sqrt{N}$ for a sufficiently large sample. In Fig. 3, we compare the results with what one would obtain neglecting selection effects: for the variance one finds a low-redshift behaviour similar to the one reported in [Hirata, Holz & Cutler \(2010b\)](#), while at high redshift selection effects become important. Likewise, at low redshift the bias is irrelevant as flux is conserved when selection effects are negligible, while above $z \simeq 8$, corresponding to the peak of the MBHB population distribution, the bias becomes strongly marked.

By fitting the numerical curves we obtained in Fig. 3, we can provide a simple analytical estimate of the lensing uncertainty (1σ deviation) as a function of redshift, in analogy to the formula provided by [Hirata, Holz & Cutler \(2010b\)](#) (eq. (20)) but now containing selection effects. We find that the following expression well fit the numerical data at all redshift (for one siren $N = 1$):

$$\begin{aligned} \sigma(\ln D^2)_{\text{fit}}^{\text{popIII}} &= 2 \left. \frac{\sigma(D)}{D} \right|_{\text{fit}}^{\text{popIII}} \\ &= \begin{cases} 0.061 \left(\frac{1-(z+1)^{-0.264}}{0.264} \right)^{1.89} & \text{for } z \leq 9.35, \\ 0.034 + 0.015 z & \text{for } z > 9.35. \end{cases} \quad (14) \end{aligned}$$

All numbers appearing in this formula have been used as

parameters for the fit, including the cut in redshift. Note that we used the same expression originally proposed in [Hirata, Holz & Cutler \(2010b\)](#) to fit the first part of the curve, finding parameter values close to the ones reported therein with a few percent global shift towards lower uncertainties which we associate to differences in the simulations of the lensing distribution between [Hirata, Holz & Cutler \(2010b\)](#) and [Takahashi et al. \(2011\)](#).⁵ At redshift higher than $z = 9.35$ we used instead a simple linear fit capturing the behaviour due to selection effects. The total fit given in eq. (14) is shown in the bottom panel of Fig. 3.

We can furthermore derive for the first time a simple analytical fit of the expected bias due to lensing on distance measurements of MBHB mergers observed by LISA. This is well fitted by the following simple polynomial function at all redshift (cf. Fig. 3):

$$\left\langle \sqrt{\mu(z)} \right\rangle_{\text{fit}}^{\text{popIII}} = 1 + 1.89 \times 10^{-6} z^{4.36}. \quad (15)$$

For completeness we provide here also the fit of the bias on distance square (cf. eq. (10)), which is identically 1 if lensing selection effects are not included:

$$\langle \mu(z) \rangle_{\text{fit}}^{\text{popIII}} = 1 + 7.125 \times 10^{-7} z^{5.124}. \quad (16)$$

By comparing the two expressions in eqs. (14) and (15) (for $N = 1$), we can find the redshift above which the lensing bias will be more significant than the lensing uncertainty (at 1σ), and thus no longer negligible for distance measurements. This happens at $z \simeq 15$. Above this redshift, the LISA distance measurement of a single MBHB merger will on average expected to be biased by lensing effects, and thus not reliable.

As the results above apply to the popIII population model only, we provide here also the fit equivalent to eq. (14) for the heavy-seed Q3 populations of [Klein et al. \(2016\)](#); [Barausse \(2012\)](#). In such case selection effects are negligible at all redshift (cf. discussion below), and we find that an optimal fit is given by

$$\sigma(\ln D^2)_{\text{fit}}^{\text{Q3}} = 2 \left. \frac{\sigma(D)}{D} \right|_{\text{fit}}^{\text{Q3}} = 0.096 \left(\frac{1 - (z+1)^{-0.62}}{0.62} \right)^{2.36}. \quad (17)$$

This is nothing but the functional form proposed by [Hirata, Holz & Cutler \(2010b\)](#) fitted to the whole redshift range up to $z = 20$, and constitutes an excellent representation of the numerical curve presented in the bottom panel of Fig. 3 (dotted line). Being selection effects negligible for heavy-seed MBHB population models, no relevant bias will appear. In other words both $\langle \mu(z) \rangle$ and $\langle \sqrt{\mu(z)} \rangle$

⁵ In particular, [Takahashi et al. \(2011\)](#) derives the PDF of magnification using a high-resolution ray-tracing numerical simulation, while [Hirata, Holz & Cutler \(2010b\)](#) employs the PDF derived in [Holz & Wald \(1998\)](#) in the context of a stochastic universe method where the geodesic deviation equation is solved backward in time with an approach similar to that used in Swiss cheese universe models.

are basically one at all redshift probed by LISA, on the contrary to what we found above for the popIII model (cf. eq. (15)).

Finally we provide results in terms of observable quantities. In the absence of an EM counterpart, a direct access to the redshift of a GW source is not possible. The quantity that is directly observable in this case is the *observed* luminosity distance of a given source (which can be converted into redshift only by assuming a cosmological model). We compute the distribution of magnification with selection effects as a function of the observed luminosity distance, eq. (6); see also Cusin, Durrer & Dvorkin (2019) for details on this derivation. In Fig. 4 we plot the number of sources from a given observed luminosity distance, visible if the magnification is μ as a function of magnification. In the bottom panel of the same figure we show the distribution of the observed magnification $\mathcal{P}_{\text{obs}}(\mu, D_{\text{obs}})$ obtained multiplying each line of the top panel by the PDF $p(\mu, D_{\text{obs}})$ obtained from Takahashi et al. (2011) converting redshift to observed distance through $D(z) = \sqrt{\mu}D_{\text{obs}}$.

Comparing the top panels of Figs. 2 and 4 it becomes apparent the role played by selection effects. The probability distribution of magnification increases as we increase the cosmological redshift of the source (for magnification μ fixed). This is a consequence of the fact that the number of sources visible from a given cosmological redshift is a monotonically increasing function of magnification. On the other hand, the number of sources visible from a given observed distance if the magnification is μ , for a fixed D_{obs} has a more involved behavior. As we vary magnification, a given bin around D_{obs} receives contributions from sources at different cosmological distances $D(z) = \sqrt{\mu}D_{\text{obs}}$. The peak of the distribution of magnification becomes broader as we increase the observed distance of a source (see bottom panel of Fig. 4), but the high-magnification tail gets suppressed. Indeed if we observe a source at very high distance, it is improbable that this is a magnified one as it would come from an even higher cosmological distance $D(z) > D_{\text{obs}}$.

This last remark may be better understood by looking at Fig. 5, which shows the mean and variance of the distance estimator as a function of observed distance. The average magnification increases from 1 as we increase D_{obs} , it reaches a peak and then goes down to values < 1 . This can be explained by looking at the MBHB redshift distribution in Fig. 1 (see also Fig. 3 in Klein et al. (2016)): being the distribution of sources peaked around redshift 8 – 10, if a source is observed from high distance it is much more probable that this is actually a source at distance $D(z) < D_{\text{obs}}$, hence a de-magnified one. On the other hand, a source at $z \lesssim 8 - 10$ has more chances to be a magnified one, as there are many sources at higher redshift with $D(z) > D_{\text{obs}}$.

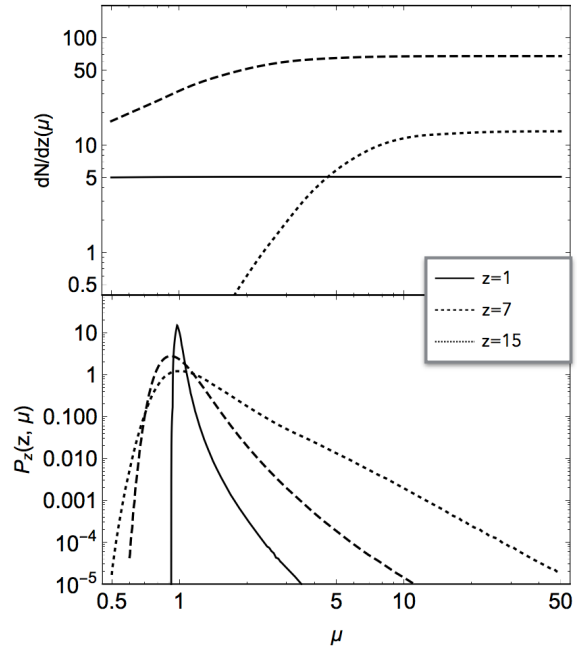


Figure 2. Top: Number of sources from a given redshift, visible if the magnification is μ as a function of magnification, see eq. (3). We assumed $T_{\text{obs}} = 4$ yr. Bottom: Distribution of magnification (cf. eq. (4)) with selection effects included. Each line is obtained multiplying the distribution $p(\mu, z)$ of Takahashi et al. (2011) by the corresponding dN/dz in the top panel (and normalising).

5 COSMOLOGICAL AND ASTROPHYSICAL IMPLICATIONS

As mentioned above, LISA MBHB standard sirens can be used to probe the expansion of the universe up to $z \sim 8$, above which EM counterparts are no longer expected to be observed (Tamanini 2017). Since we found that selection effects mainly affect the MBHB distance measurements at $z \gtrsim 10$, we do not expect them to bias LISA standard siren analyses. In fact, by using a similar procedure to the one outlined in Speri et al. (2020), we checked that Λ CDM cosmological parameters will not be biased for any realistic number of MBHB standard sirens that LISA will observe. Furthermore, by using eq. (14) for LISA MBHB lensing uncertainty measurements, we find that forecasts on Λ CDM parameters are consistent with previous results. Constraints on Λ CDM are only marginally better than the one reported in the literature (Tamanini 2017; Belgacem et al. 2019; Speri et al. 2020) (differences are due to the slightly better fit provided by eq. (14) with respect to the one of Hirata, Holz & Cutler (2010b)). Selection effects could however affect other cosmological measurements based on weak lensing measurements with standard sirens, such as for example cross-correlations with EM matter surveys (Congedo & Taylor 2019). The impli-

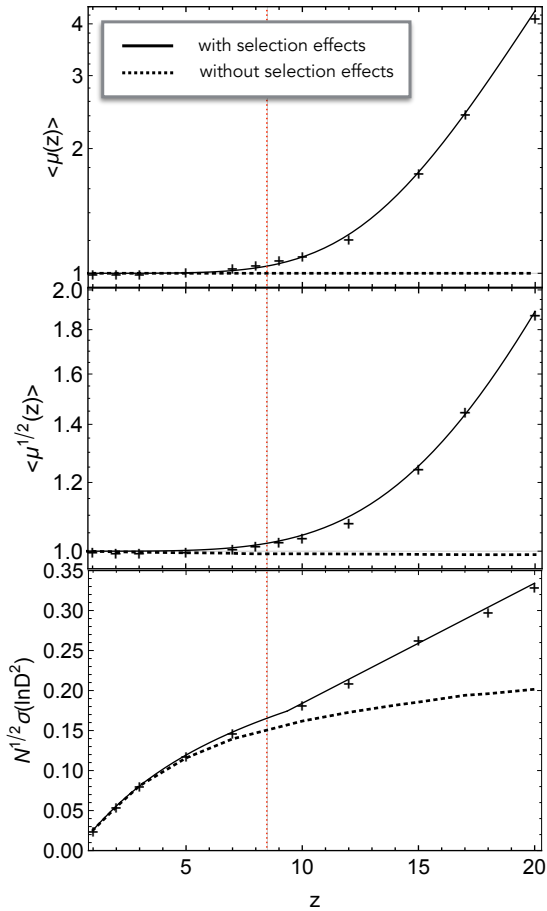


Figure 3. Bias and uncertainty of the distance estimator \hat{D} as a function of cosmological redshift. We show both the bias on distance and on distance square, $\langle \mu^{1/2} \rangle$ and $\langle \mu \rangle$, respectively. We explicitly show the effect of including selection effects in the analysis: $\langle \mu \rangle$ is identically one if selection effects are not included as a consequence of flux conservation. The solid lines are the fitting formulae in eqs. (14) and (15). With a vertical red line we indicate the maximum redshift at which for our astrophysical model, an EM counterpart is observable.

cations on such analyses are however more complicated to assess and their investigation will be left for future studies.

Important implications due to lensing selection effects will instead arise in MBHB population studies. The redshift dependence of the MBHB merger rate yields information on the processes shaping the evolution and growth of the MBHB population, their environment and their relation with galaxy assembly (see e.g. Haehnelt (1994); Kauffmann & Haehnelt (2000); Volonteri, Haardt & Madau (2003); Enoki et al. (2004); Sesana et al. (2005); Micic et al. (2007); Barausse (2012); Colpi (2014); Umeda et al. (2016); Valiante et al. (2016)). Reconstructing the redshift and mass distribution of MBHB mergers constitutes thus an important scientific objective for the LISA mission (Sesana, Volonteri & Haardt 2007; Sesana

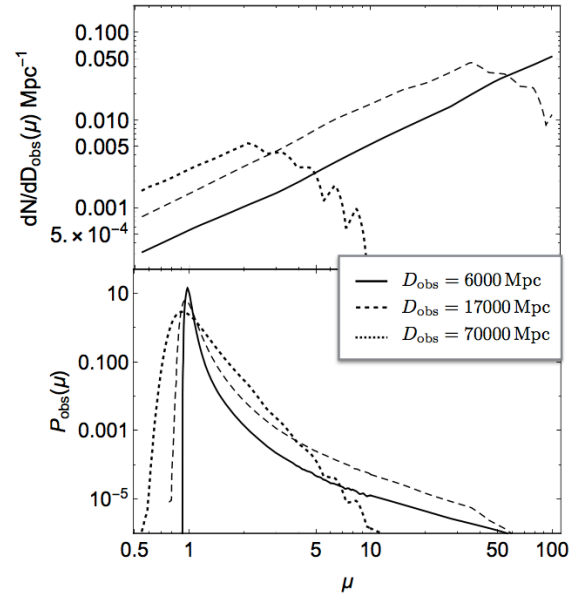


Figure 4. Top: Number of sources from a given observed luminosity distance, visible if the magnification is μ as a function of magnification (cf. eq. (6)). We assumed $T_{\text{obs}} = 4$ yr. Bottom: Distribution of magnification (4) with selection effects included. Each line is obtained multiplying the distribution $p(\mu, D_{\text{obs}})$ computed from the simulation of Takahashi et al. (2011) by the corresponding dN/dD_{obs} in the top panel (and normalising).

et al. 2011; Colpi et al. 2019). Such reconstructions will be performed by fitting merger rate distribution models to the MBHBs detected by LISA, in analogy to analyses for stellar-mass black hole binaries currently implemented with LIGO-Virgo observations (Fishbach, Holz & Farr 2018), which have already been shown to be affected by lensing selection effects; see e.g. Dai, Venumadhav & Sigurdson (2017); Oguri (2018). Since these analyses will require a sampling in redshift (and mass) of the LISA MBHB merger distribution, the effect of the bias on the distance estimator becomes in this case important. The reason is that, although we have a high statistics of events and the bias on the distance estimator is independent on the sample size, the variance of the distance measurement associated to each bin decreases with \sqrt{N} . In figure 6 we compare bias and uncertainty for the sample of sources with $\text{SNR} > 8$ (computed here neglecting lensing), as a function of the observed redshift (derived from the D_{obs} assuming our fiducial cosmology). For this figure we present results for all three models considered in Klein et al. (2016): popIII and the other two heavy-seed Q3 MBH population models (with and without delays between galaxy merger and MBHB merger, respectively “Q3-d” and “Q3-nd”). We see that for popIII and Q3-nd, the bias is always bigger than the uncertainty at almost all observed redshift of interest. This implies that all

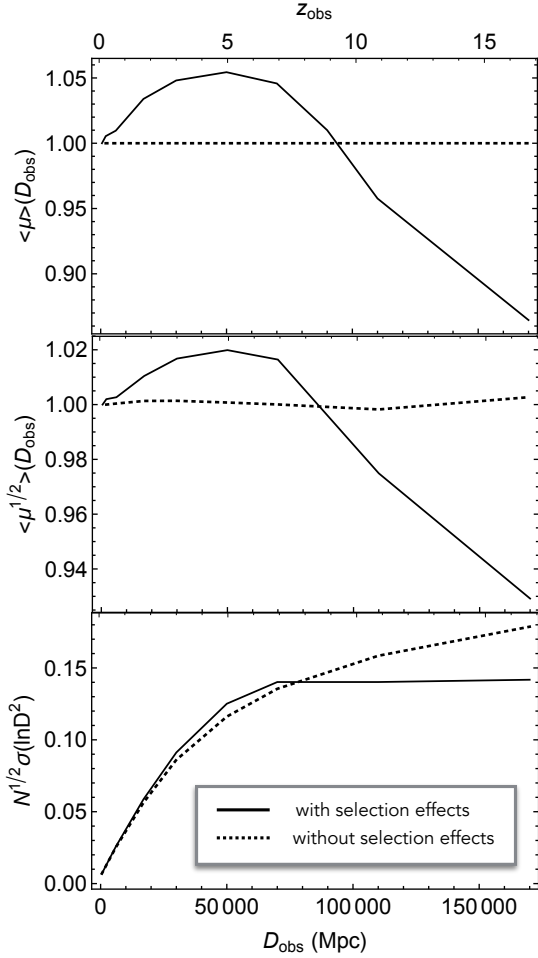


Figure 5. Bias and uncertainty of the distance estimator \hat{D} as a function of the observed luminosity distance (here z_{obs} is derived from $D(z_{\text{obs}}) = D_{\text{obs}}$ assuming our fiducial cosmology). We show both the bias on distance and on distance square, $\langle \mu^{1/2} \rangle$ and $\langle \mu \rangle$, respectively. We explicitly show the effect of including selection effects in the analysis.

analyses based on a sampling in z_{obs} or D_{obs} are expected to be strongly biased by lensing selection effects. Further work is thus required to understand how to deal with this bias and be able to extract relevant astrophysical information from the LISA redshift distribution of MBHB mergers. In the Q3-d scenario instead, lensing selection effects will have negligible implications on any population study as the bias will always be lower than the uncertainty of each redshift/distance bin. This is due to the lower number of sources detected by LISA in the Q3-d model (cf. Klein et al. (2016)) which implies that $\sigma_{\text{obs}}/\sqrt{N(z_{\text{obs}})}$ remains sufficiently big. Note finally that these results are based on an observational time of 4 years, while a possible extension up to 10 years is envisaged for the LISA mission (Amaro-Seoane et al. 2017). For longer observational periods we expect the

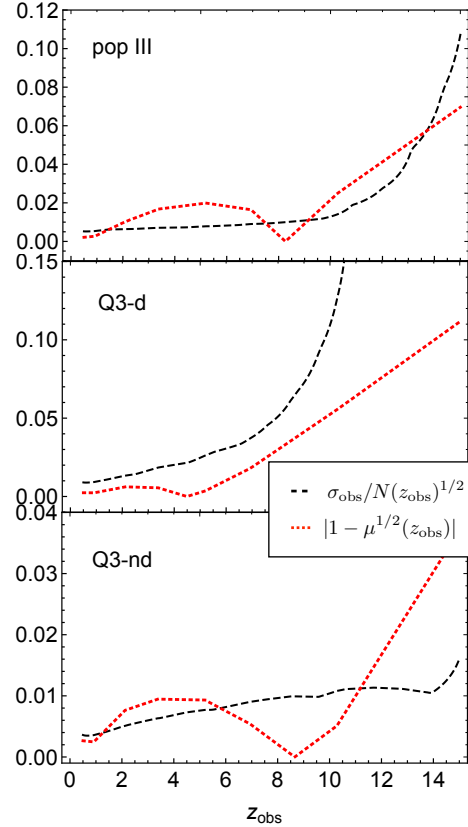


Figure 6. Comparison between bias and (relative) uncertainty $\sigma_{\text{obs}} = \sigma(\ln D)(z_{\text{obs}})$ on the distance estimator, as function of the observed redshift, for the three astrophysical models under study. The uncertainty at a given distance scales with the square root of the number density of detectable sources from that distance. We assumed a mission lifetime of 4 years.

results above to show an even more marked bias due to lensing selection effects, as $N(z_{\text{obs}})$ will on average grow linearly with the observational time.

6 DISCUSSION AND CONCLUSION

We have presented a method to assess the effect of weak and strong lensing on the estimation of the luminosity distance for a population of astrophysical GW sources, taking into account selection effects due to the finite sensitivity of a GW detector. Since a realistic GW detector has a finite horizon, the probability that a source detected at redshift z is magnified is higher than the probability that it is demagnified. As a consequence, the mean of the distribution of magnification for sources at sufficiently high redshift, is shifted from 1 to higher values. These effects, which we dubbed *lensing selection effects*, disappear in the limit of a

perfect instrument (or analogously, in the limit of sources at redshift much lower than the instrument horizon).⁶

Although this fact was already pointed out in the literature, see e.g. the discussion section of [Hirata, Holz & Cutler \(2010b\)](#), this is the first place where a quantitative estimate of the selection effects on the determination of the luminosity distance of MBHB has been presented. In particular we provide an unbiased estimator for the luminosity distance as a function of redshift, which includes the effect of lensing magnification. We explicitly studied the case of a population of MBHB mergers visible by LISA. Fixing the reference astrophysical model to the popIII source distribution of [Barausse \(2012\)](#); [Klein et al. \(2016\)](#), we computed the bias and the variance of the distance for the entire population (with or without EM counterpart).

While the effect of the bias on the distance estimator for sources with EM counterpart is typically below the variance threshold, it may become relevant for high redshift sources when the statistics of detectable events is large. If no EM counterpart is present, a more useful quantity to look at is the distribution of magnification as function of observed distance. We compare the mean magnification to the variance as function of observed distance in [Fig. 6](#). This comparison shows that sources observed from high distances, specifically beyond the peak of the merger distribution, are on average de-magnified and that the average magnification is typically larger than the associated variance, hence it should not be neglected when working out distance estimates with a statistical approach, such as for example in source population studies and in particular to determine the merger rate as a function of redshift.

Notice however that our estimate of the variance of luminosity distance used the Cramer-Rao bound, as explained in [Sec. 3](#). A more realistic analysis would estimate the variance of luminosity distance as the second moment of [eq. \(9\)](#), re-running a ray-tracing simulation taking into account wave effects in the PDF of lensing magnification. For this reason the value of redshift at which bias and variance are comparable in value may be underestimated in our analysis. Notice however that the scope of this paper is to point out the methodology to follow in future realistic lensing studies and not to provide precise and conclusive estimates. Moreover one of the main results of our prelim-

inary analysis is that for standard sirens the lensing bias is always within the variance level. This is a conservative result as we use the Cramer-Rao bound to compute the variance of luminosity distance and a more realistic analysis would typically give a an estimated value of the variance above the Cramer-Rao bound. In other words, a more realistic study would find that for standard sirens lensing bias is still be within the estimated variance level.

As mentioned above, we focused our investigations on the popIII MBHB population model considered in [Barausse \(2012\)](#); [Klein et al. \(2016\)](#). We made this choice because the popIII model is the one for which the implications of the selection effects are higher. For the other heavy-seed MBHB population models of [Barausse \(2012\)](#); [Klein et al. \(2016\)](#), lensing selection effects are less relevant since their redshift distributions are shifted towards lower redshift values and their mass distribution towards higher masses. Because of this almost all heavy-seed MBHB merger events are detectable by LISA ([Klein et al. 2016](#)), and a few sub-threshold events have the probability of being magnified enough to result detectable. We also showed that only for the heavy seed Q3-nd model of [Barausse \(2012\)](#); [Klein et al. \(2016\)](#) population studies will be biased by selection effects, while for the Q3-d model no such bias should arise (cf. [Fig. 6](#)). As explained above, this is due to the higher number of LISA detection in Q3-nd with respect to Q3-d which drives the distance uncertainty on the luminosity distance estimator given by [eq. \(11\)](#) to lower values. Additionally we remark that our result for the distribution of magnification are taken from the ray-tracing simulation of [Takahashi et al. \(2011\)](#), which does not include the effect of baryons. The inclusion of baryons typically enhances the high-magnification tail of the distribution. Our results of lensing selection effects should therefore be taken as conservative estimates.

For the benefit of future investigations, we also supplied here simple analytical expressions for the lensing distance error containing for the first time the contribution due to selection effects. These ready-to-use expressions can be employed in LISA MBHB analyses requiring realistic distance determination of each source. The clearest example of such analyses is provided by cosmological studies with standard sirens, which will need to take into account the effect of lensing on the luminosity distance errors as this is on average always dominant with respect to LISA instrument uncertainties at high redshift, even if, as we showed, lensing selection effects appear to be irrelevant at the redshift range over which EM counterpart to MBHB mergers are expected to be observed.

In this work, we assumed to know the underlying distribution of sources, and we estimated the bias in the reconstruction of distance distribution, induced by lensing selection effects. Of course, in realistic population studies, one rather wants to infer the (unknown) properties of a given source population, starting from an observed sample of sources. To be concrete, let us assume that one wants to extract the merger rate per unit chirp mass and cosmological redshift, from the observed rate. Then one should use

⁶ We stress that our derivation of lensing selection effects relies on the geometric optics approximation. We expect wave effects to become non-negligible in the LISA waveband only when dealing with diffusion off sub-galactic structures, see e.g. [Takahashi & Nakamura \(2003\)](#); [Nakamura \(1998\)](#); [Takahashi \(2017\)](#); [Dolan \(2008\)](#); [Cusin, Durrer & Ferreira \(2019\)](#); [Cusin & Lagos \(2020\)](#); [Dalang, Cusin & Lagos \(2021\)](#). Diffraction on sub-galactic scales makes lenses on those scales effectively transparent to GW in the LISA band ([Takahashi & Nakamura 2003](#)), in contrast with what happens for lensing of EM sources (see e.g. [Fleury, Larena & Uzan \(2015\)](#)) as the EM spectrum is at much lower wavelengths than any relevant astrophysical structure at cosmological scales.

that the two distributions are related by (fixing a reference observation time)

$$\begin{aligned} \frac{d^2 N(\mathcal{M}_{\text{obs}}, z_{\text{obs}})}{d\mathcal{M}_{\text{obs}} dz_{\text{obs}}} &= \\ &= \int d \ln \mu \frac{d\mathcal{P}_z(\mu, z)}{d \ln \mu} \frac{d^2 N(\mathcal{M}, z)}{d\mathcal{M} dz} \left| \frac{\partial(\mathcal{M}, z)}{\partial(\mathcal{M}_{\text{obs}}, z_{\text{obs}})} \right|, \end{aligned} \quad (18)$$

where $\mathcal{M}_{\text{obs}}(1 + z_{\text{obs}}) = \mathcal{M}(1 + z)$ and the Jacobian (at fixed μ) is given by

$$\left| \frac{\partial(\mathcal{M}, z)}{\partial(\mathcal{M}_{\text{obs}}, z_{\text{obs}})} \right| = \frac{(1 + z_{\text{obs}})}{(1 + z)} \frac{D'(z_{\text{obs}})}{D'(z)} \frac{D(z)}{D(z_{\text{obs}})}. \quad (19)$$

We observe that in eq. (18), $\mathcal{P}_z(\mu, z)$ is the observed distribution of magnification, with selection effects included (cf. eq. (5)), which in turn depends on mass and redshift distribution of sources. In analyses with real observational data, it is the right hand side of eq. (18), considered as function of source-frame chirp mass and cosmological redshift, that has to be fitted to the observed rate to extract information on the intrinsic redshift and mass distribution of the population under study. Studies along these lines for the case of ground-based detectors have been considered for example by Dai, Venumadhav & Sigurdson (2017); Oguri (2018).

To conclude, lensing of high-redshift GW sources biases the observed GW signal, hence contaminating the reconstruction of the astrophysical properties of the population of emitting sources (above of all distances and source-frame chirp masses). For high-redshift GW sources, the characterisation of all the implications due to lensing, including selection effects due to the specifics of a given instrument, is thus of paramount importance, not only to infer in an accurate way their astrophysical properties across cosmic time, but also to be able to use high-redshift GW sources as a new compelling cosmological probe.

Acknowledgements. We are very grateful to Ruth Durrer and Irina Dvorkin for valuable discussions during different stages of this project. We also thank Enrico Barausse, Enis Belgacem, Giuseppe Congedo, Daniel Holz, Francesca Lepori and Jean-Philippe Uzan for discussions and comments on the manuscript. GC thanks Alessandra Buonanno and the entire Astrophysical and Cosmological Relativity division at the Max Planck Institute for Gravitational Physics (Albert Einstein Institute) in Potsdam for their warm hospitality during the first stage of this work. The work of GC is supported by the Swiss National Science Foundation.

Data Availability Statement. The data underlying this article will be shared on reasonable request to the corresponding author.

APPENDIX A: BOUNDING THE VARIANCE WITH THE FISHER INFORMATION

Let us assume to have an unknown deterministic parameter x to be estimated from N independent observations of X , each distributed following a probability density function $f(x, X)$. The variance of any unbiased estimator \hat{x} of x is bounded by the reciprocal of the Fisher information

$$\text{var}(\hat{x}) \geq \frac{1}{I(x)}, \quad (A1)$$

where

$$I(x) = N \int dx f(x, X) \left(\frac{d}{dx} f(x, X) \right)^2. \quad (A2)$$

If we have a biased estimator \hat{T} whose expectation value is not x but a finite function $\psi(x)$ of it, the bound is

$$\text{var}(\hat{T}) \geq \frac{|\psi'(x)|^2}{I(x)}, \quad (A3)$$

where $\psi'(x) = \partial\psi/\partial x$. Let us use this result in our context. Let us fix a given redshift z and assume that we have $N(z)$ measurements of luminosity distance from a given bin around z . We pose $x = \ln \mu$ and $\hat{T} = \hat{D}^2$ with $\hat{D}^2 \equiv \mu \bar{D}_{\text{obs}}^2 = e^x \bar{D}_{\text{obs}}^2$. Then using (A3), we get the following upper bound on the variance of the distance estimator

$$\text{var}(\hat{D}^2) \geq \frac{(\hat{D}^2)^2}{I(x)}, \quad (A4)$$

where

$$I(x) = N(z) \int dx \mathcal{P}_z(x, z) \left(\frac{d}{dx} \mathcal{P}_z(x, z) \right)^2, \quad (A5)$$

and the dependence on z on the left hand side is understood. Following the same reasoning, but considering $\hat{T} = \ln \hat{D}^2 \equiv \ln \bar{D}_{\text{obs}}^2 + x$, we have

$$\text{var}(\ln \hat{D}^2) \geq \frac{1}{I(x)}. \quad (A6)$$

REFERENCES

- Abbott B., et al., 2017a, Phys. Rev. Lett., 119, 161101
 Abbott B. P., et al., 2016a, Phys. Rev., X6, 041015, [erratum: Phys. Rev.X8,no.3,039903(2018)]
 Abbott B. P., et al., 2016b, Phys. Rev. Lett., 116, 241103
 Abbott B. P., et al., 2016c, Phys. Rev. Lett., 116, 061102
 Abbott B. P., et al., 2017b, Phys. Rev. Lett., 118, 221101, [Erratum: Phys. Rev. Lett.121,no.12,129901(2018)]
 Abbott B. P., et al., 2017c, Astrophys. J., 851, L35
 Abbott B. P., et al., 2017d, Phys. Rev. Lett., 119, 141101
 Abbott B. P., et al., 2019, Phys. Rev., X9, 031040
 Abbott R., et al., 2020
 Ajith P. et al., 2007, Classical and Quantum Gravity, 24, S689
 Amaro-Seoane P., et al., 2017
 Barausse E., 2012, Mon. Not. Roy. Astron. Soc., 423, 2533

- Belgacem E., et al., 2019, JCAP, 07, 024
- Bonetti M., Sesana A., Haardt F., Barausse E., Colpi M., 2019, Mon. Not. Roy. Astron. Soc., 486, 4044
- Cai R.-G., Tamanini N., Yang T., 2017, JCAP, 05, 031
- Calcagni G., Kuroyanagi S., Marsat S., Sakellariadou M., Tamanini N., Tasinato G., 2019a, Phys. Lett. B, 798, 135000
- Calcagni G., Kuroyanagi S., Marsat S., Sakellariadou M., Tamanini N., Tasinato G., 2019b, JCAP, 10, 012
- Caprini C., Tamanini N., 2016, JCAP, 10, 006
- Colpi M., 2014, Space Sci. Rev., 183, 189
- Colpi M., et al., 2019
- Congedo G., Taylor A., 2019, Phys. Rev. D, 99, 083526
- Corman M., Escamilla-Rivera C., Hendry M., 2020
- Cusin G., Durrer R., Dvorkin I., 2019
- Cusin G., Durrer R., Ferreira P. G., 2019, Phys. Rev. D, 99, 023534
- Cusin G., Lagos M., 2020, Phys. Rev. D, 101, 044041
- Dai L., Venumadhav T., Sigurdson K., 2017, Phys. Rev., D95, 044011
- Dalang C., Cusin G., Lagos M., 2021
- Dayal P., Rossi E. M., Shiralilou B., Piana O., Choudhury T. R., Volonteri M., 2019, MNRAS, 486, 2336
- Dolan S. R., 2008, Phys. Rev., D77, 044004
- Enoki M., Inoue K. T., Nagashima M., Sugiyama N., 2004, Astrophys. J., 615, 19
- Finn L. S., Chernoff D. F., 1993, Phys. Rev., D47, 2198
- Fishbach M., Holz D. E., Farr W. M., 2018, Astrophys. J. Lett., 863, L41
- Fleury P., Larena J., Uzan J.-P., 2015, Journal of Cosmology and Astroparticle Physics, 2015, 022
- Haehnelt M. G., 1994, Mon. Not. Roy. Astron. Soc., 269, 199
- Hilbert S., Gair J. R., King L. J., 2011, Mon. Not. Roy. Astron. Soc., 412, 1023
- Hirata C. M., Holz D. E., Cutler C., 2010a, Phys. Rev. D, 81, 124046
- Hirata C. M., Holz D. E., Cutler C., 2010b, Physical Review D, 81
- Holz D. E., Hughes S. A., 2005, Astrophys. J., 629, 15
- Holz D. E., Linder E. V., 2005, Astrophys. J., 631, 678
- Holz D. E., Wald R. M., 1998, Phys. Rev. D, 58, 063501
- Katz M. L., Kelley L. Z., Dosopoulou F., Berry S., Blecha L., Larson S. L., 2020, Mon. Not. Roy. Astron. Soc., 491, 2301
- Kauffmann G., Haehnelt M., 2000, Mon. Not. Roy. Astron. Soc., 311, 576
- Klein A., et al., 2016, Phys. Rev. D, 93, 024003
- Maggiore M., 2007, Gravitational Waves. Vol. 1: Theory and Experiments, Oxford Master Series in Physics. Oxford University Press
- Micic M., Holley-Bockelmann K., Sigurdsson S., Abel T., 2007, Mon. Not. Roy. Astron. Soc., 380, 1533
- Mukherjee S., Wandelt B. D., Silk J., 2020, Monthly Notices of the Royal Astronomical Society, 494, 1956–1970
- Nakamura T. T., 1998, Phys. Rev. Lett., 80, 1138
- Oguri M., 2018, Mon. Not. Roy. Astron. Soc., 480, 3842
- Robson T., Cornish N. J., Liu C., 2019, Classical and Quantum Gravity, 36, 105011
- Salcido J., Bower R. G., Theuns T., McAlpine S., Schaller M., Crain R. A., Schaye J., Regan J., 2016, Mon. Not. Roy. Astron. Soc., 463, 870
- Sato M., Hamana T., Takahashi R., Takada M., Yoshida N., Matsubara T., Sugiyama N., 2009, The Astrophysical Journal, 701, 945
- Schutz B. F., 1986, Nature, 323, 310
- Sereno M., Jetzer P., Sesana A., Volonteri M., 2011, Mon. Not. Roy. Astron. Soc., 415, 2773
- Sereno M., Sesana A., Bleuler A., Jetzer P., Volonteri M., Begelman M., 2010, Phys. Rev. Lett., 105, 251101
- Sesana A., Gair J., Berti E., Volonteri M., 2011, Phys. Rev. D, 83, 044036
- Sesana A., Haardt F., Madau P., Volonteri M., 2005, Astrophys. J., 623, 23
- Sesana A., Volonteri M., Haardt F., 2007, Mon. Not. Roy. Astron. Soc., 377, 1711
- Shang C., Haiman Z., 2010, Monthly Notices of the Royal Astronomical Society, 411, 9–22
- Speri L., Tamanini N., Caldwell R. R., Gair J. R., Wang B., 2020
- Takahashi R., 2017, Astrophys. J., 835, 103
- Takahashi R., Nakamura T., 2003, Astrophys. J., 595, 1039
- Takahashi R., Oguri M., Sato M., Hamana T., 2011, Astrophys. J., 742, 15
- Tamanini N., 2017, J. Phys. Conf. Ser., 840, 012029
- Tamanini N., Caprini C., Barausse E., Sesana A., Klein A., Petiteau A., 2016, JCAP, 04, 002
- Umeda H., Hosokawa T., Omukai K., Yoshida N., 2016, Astrophys. J. Lett., 830, L34
- Valiante R., Schneider R., Volonteri M., Omukai K., 2016, MNRAS, 457, 3356
- Volonteri M., Haardt F., Madau P., 2003, ApJ, 582, 559